Multiplexed Hydrogel Microparticle Suspension Arrays for Facile Ribosomal RNA Integrity Assays

A thesis submitted by

Yader E. Duenas

in partial fulfillment of the requirements for the degree of

Master of Science
in
Bioengineering

TUFTS UNIVERSITY

May 2015

ADVISER:
Hyunmin Yi, Ph.D.

Abstract

Reliable RNA integrity assay is important for a wide range of applications in genomics and diagnostics, yet the existing technologies have certain limitations such as large amount of sample required, high cost of equipment and/or long turnaround times. I report a simple assay method to analyze bacterial ribosomal RNA (rRNA) from complex total RNA samples utilizing shape-encoded and single-stranded DNA-conjugated hydrogel microparticle suspension arrays with no need for target amplification and under standard fluorescence imaging conditions. I show that this simple microparticle-based sensing scheme is reliable, sequence-specific and presents a responsive binding behavior to target RNA concentrations. Moreover, the relative stability of 16S and 23S rRNA can be assessed in a simple shape encoding-based multiplexed format. Combined, these findings represent a significant step toward cheap, fast, simple, and reliable assays for the analysis of rRNA and general RNA integrity.

Acknowledgments

Through these acknowledgements I want to extend my most sincere gratitude to those who have provided assistance, insight, and motivation in order to make this research possible. Without their incredible help this work could not be finished.

First and foremost, I would like to acknowledge my adviser and academic father, Professor Hyunmin Yi, for his continuous guidance, patience and encouragement.

I would also like to thank my dissertation committee members, Professor Qiaobing Xu and Professor Ayse Asatekin, for their commitment and interest in my research. I appreciate they took time of their busy schedule to participate on my committee. I am grateful for the support of the Yi lab members, especially Sukwon Jung, JaeHun Lee, and Cuixian Yang.

I would like to sincerely thank my family for their everlasting support and patience. Especially, I thank my Boston family (Gladys, Cesar, Cristina and Alejandro) for receiving me with open arms and supporting me through this endeavor. Thanks to my mother, Andrea, and my siblings, Edwin and Any, for sending love and support from Peru. Lastly, to my late father thank you for showing me the value of perseverance.

Table of Contents

List of Figures

Chapter 1: Introduction

1.1 Significance

Determining the quality of extracted RNA samples is important prior to performing a wide range of applications including gene expression analysis, clinical and other diagnostics.[1-5] RNA samples with poor quality can affect not only the reliability of the assays but also increase the cost of the already expensive and time-consuming procedures. Even though many methods for RNA isolation from cells and tissues have improved recently,[6, 7] there exist limitations in the methodologies used to assess the RNA quality in a specific and reliable manner from complex mixtures as in total RNA samples.

By definition, RNA quality includes the analysis of RNA purity and RNA integrity.[8, 9] Purity is most commonly assessed by measuring the UV absorbance ratios at different wavelengths, *i.e.* A_{260}:A_{280} and A_{260}:A_{230} to determine possible contaminations including proteins and phenol, guanidine and others respectively.[10, 11] Due to the labile nature of RNA and the ubiquitous presence of ribonucleases (RNases) in the environment, the analysis of integrity is also essential to determine if the RNA molecules are intact or have been degraded to small fragments. Often in *E. coli* and bacterial cells the 23S:16S ratio of ribosomal RNA (rRNA) is used as the primary indicator to qualify the integrity of RNA, a ratio of 2.0 being representative of intact RNA.[11]

1.2 Challenges

Agarose gel electrophoresis has been traditionally utilized to characterize RNA and to analyze the integrity of the samples by comparing the intensity of the rRNA bands; however there exist several limitations including the significant amount of RNA (on the order of 0.5-2 μg)[12] necessary to visualize the bands and the use of toxic chemicals such as ethidium bromide and formaldehyde that require special handling and treatment. A common alternative is to use commercial instruments that are based on the microfluidic capillary electrophoresis technology and automated systems to report standardized RNA quality values like the RNA Integrity Number (RIN)[13] or the RNA Quality Indicator (RQI)[14]. This technique requires very small amount of samples and offers more accurate determination of the RNA integrity, but suffers from high equipment cost and long turnaround times.[15] There are more alternatives being used as proof-of-principle for rRNA sensing that are capable of separately detecting 16S and 23S rRNA. For instance, the use of base complementarity to capture specific RNA sequences stands out among other techniques. For this purpose, some studies relied on the use of tools like peptide nucleic acids (PNA),[16] metal-enhanced fluorescence,[17] surface plasmon resonance imaging[18] among others.[19-21] However, they have been limited to work with synthetic RNA sequences and still require special equipment and expensive probe designs.

In addition, commonly utilized planar platforms such as microarrays require long incubation and processing time due to nonspecific binding and slow

hybridization kinetics,[22] as well as the needs for signal amplification through polymerase chain reaction (PCR) due to low target titer and limited RNA stability.[23] In contrast, hydrogel microparticles as platforms offer a number of advantages including rapid solution-like kinetics, selective binding due to hydrophilic nature of the probe platforms, and the potential for rapid and high throughput analysis in microfluidic scanner setups.[24, 25]

Combined, there exists an unmet need for a simple, reliable and inexpensive assay method that is sensitive, specific and could work in a multiplexed format to examine the RNA integrity without the need of complex equipment or extensive procedures.

1.3 Research Approach

In order to tackle these challenges, I utilize simple shape-encoded polymeric hydrogel microparticles in a suspension array format, as shown in Fig. 1. Specifically, the microparticles containing single-stranded (ss) DNA probes are fabricated in a robust replica molding scheme as shown in Fig. 1(A). For this, PDMS micromolds are filled with a preparticle solution containing polymerizable poly(ethylene glycol) diacrylate (PEGDA) and Acrydite^{TM}-modified ssDNA, which possesses an acrylamide group that allows for copolymerization with other acrylate monomers,[26] and then exposed to UV light to be polymerized by photoinduced radical polymerization.[27] The as-prepared microparticles are checked to confirm the incorporation of the ssDNA probes by DNA-DNA hybridization with fluorescein-labeled ssDNA as shown in the fluorescence

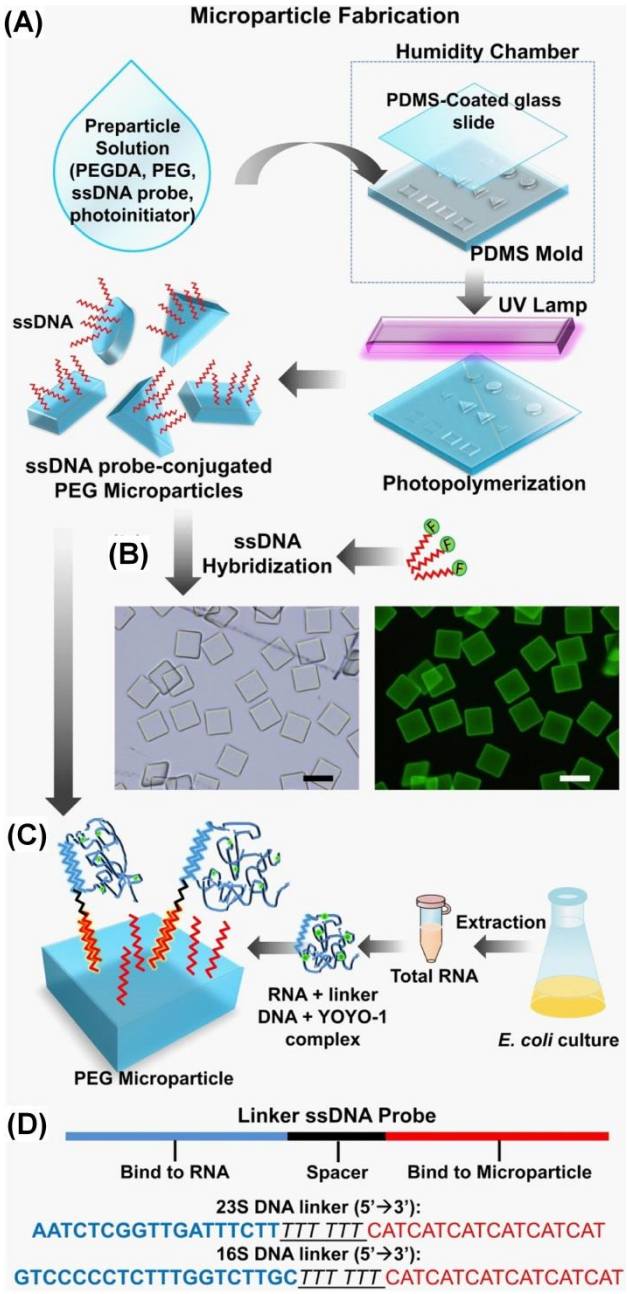

Fig. 1. (A) ssDNA-incorporated PEGDA microparticle fabrication via replica molding. (B) Brightfield and fluorescence micrographs upon hybridization with fluorescein-labeled ssDNA. (C) rRNA capture assay with microparticles, using total RNA samples extracted from *E. coli* cells. (D) Design of linker DNA sequences used to target 16S/23S rRNA molecules.

micrograph in Fig. 1.B. These microparticles are then incubated with total RNA samples that are extracted from *E. coli* culture and pre-mixed with a linker DNA and an intercalating agent YOYO-1 dye, as shown in the schematic diagram of Fig. 1.C. The design of the linker DNA is shown in Fig. 1.D, and consists of a region complementary to the target rRNA,[28, 29] a spacer, and a region complementary to the capture DNA on the microparticles. Specifically, I utilized the rrsH 16S rRNA region and the rrlH 23S rRNA region of rrnH operon as described by Fuchs *et al*.[30]

In this report, I demonstrate a simple and reliable rRNA capture assay from total RNA samples using shape-encoded ssDNA-conjugated polymeric hydrogel microparticles in a sandwich assay format, without the need of target amplification and under standard fluorescence imaging conditions. First, I show that this simple microparticle assay is reliable and sequence-specific to the rrsH region of 16s rRNA of an *E. coli* BL21 strain. Second, I examine the responsiveness of the microparticle assays with varying concentrations of the total RNA samples, and establish quantitative binding behavior. Finally, relative stability of 16S and 23S rRNA are examined in a simple shape-encoded multiplexed scheme. Combined, these results represent a major step toward reliable and quantitative ribosomal RNA and general RNA sample stability assays with low volume microparticle suspension arrays without the need for electrophoretic separation, sample amplification or costly equipment.

Chapter 2: Background

2.1 Ribonucleic Acid

2.1.1 Structure and rRNA

Ribonucleic acid (RNA) is a polymeric macromolecule that intervenes in several of the process related to gene expressions along with DNA. From the chemical standpoint, RNA differs from DNA in the presence of a uracil base replacing the thymine base and the presence of an OH group attached to the second carbon of the ribose sugar. Under certain conditions like pH or metal ions presence, this OH group can react with the phosphodiester bond thus the labile nature of RNA.[31]

Molecules such as messenger RNA (mRNA), transfer RNA (tRNA) and ribosomal RNA (rRNA) have a very well-known and important role in protein synthesis.[32] Approximately 80% of total RNA in *E. coli* cells corresponds to rRNA and 15% to tRNA, these RNA molecules are usually protected in the cell by chemical modifications (e.g. amino acylation for tRNA) and by complexing with ribosomal proteins (rRNA in the ribosome).[33] In fact, rRNA represents 60% (w/w) of the material in the ribosomes. In bacterial cells the ribosomes present two subunits: the 50S and 30S respectively. The large 50S subunit contains the 23S and 5S rRNA, while the small 30S subunit is formed by the 16S rRNA. A model for the 16S and 23S rRNA structure is shown in Fig. 2.

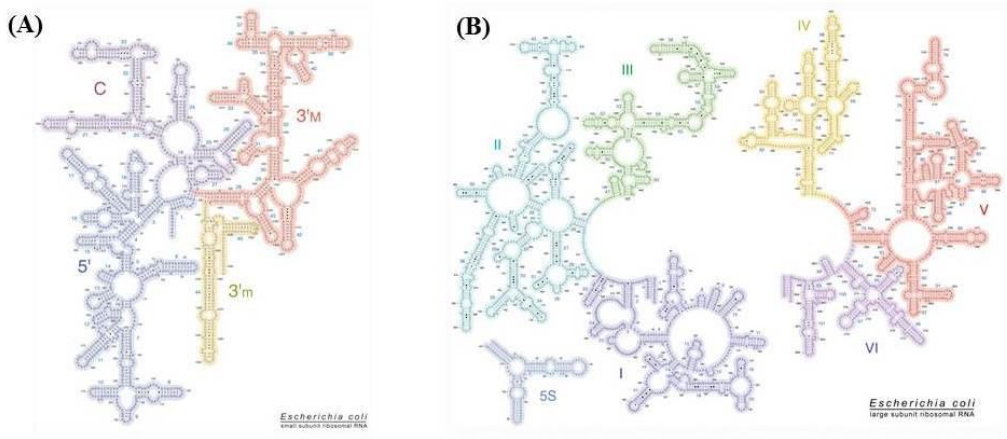

Fig. 2. (A) Secondary structure of *E. coli* 16S rRNA (B) Secondary structure of *E. coli* 23S rRNA. This figure was reproduced from http://rna.ucsc.edu/ [34]

2.1.2 16S and 23S rRNA relationship

The transcription of rRNA in E. coli is controlled by promoters that are considered among the strongest in the cell. rRNA transcription is also considered the rate-limiting step in the ribosome biosynthesis.[35] Fig. 3 shows the general organization of the seven rRNA operons in E. coli indicating the promoters and terminators. The fact that the 16S and 23S rRNA are derived from the same set of promoters, indicates that they are present in the same number in the cell.

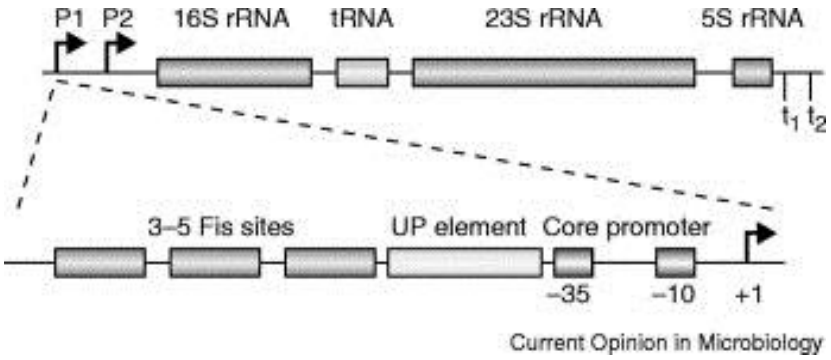

Fig 3. Diagram for rRNA operons in *E. coli*. Transcript contains the three rRNA species transcribed from promoters *rrn* P1 and *rrn* P2. This figure was reproduced from Scheider et al.[35]

Traditionally, the gold standard for the measurement of RNA integrity in bacterial cells has been the ratio of 23S and 16S rRNA bands obtained from agarose gel electrophoresis. Specifically, for an intact RNA sample the 23S rRNA band has twice the intensity of the 16S rRNA band. Since the 23S and 16S molecules are present in a 1:1 ratio, the ratio of 2.0 for the band intensities is in direct relationship with the average number of nucleotides forming each molecule. The average number of intercalating agent molecules that bind to 23S and 16S rRNA molecules is also in a 2:1 relation. Values higher than 1.8 are often considered representative of RNA samples of high quality.[11]

2.1.3 RNA quality assessments

Research and applications of many molecular biology techniques place strong emphasis in working with high quality RNA samples; here two of the most common techniques used to asses this problem are briefly described.

2.1.3.1 Agarose Gel Electrophoresis

Gel electrophoresis relies on the difference in electrophoretic mobility of the distinct rRNA molecules. Total RNA samples are loaded into an agarose gel and forced to pass through the crosslinked gel network by applying determined voltage. The different fragments are then visualized by the addition of an intercalating agent such as ethidium bromide and exposing the gel to UV light.[11] The standard method to characterize the quality of each sample from bacterial cells is by comparing the intensities of the bands corresponding to the 16S and 23S rRNA, since these sequences are highly conserved, and their sizes

are approximately in 1:2 ratio, respectively. Even though gel electrophoresis is an inexpensive technique and allows identifying the presence of the rRNA fragments, it is not a very sensitive technique and requires large amounts of sample to be loaded to the gel. Also, the use of intercalating agents to bind to nucleic acids samples is considered mutagenic and should be handled with extreme caution.

2.1.3.2 Capillary Gel Electrophoresis

This technique is based on the same principle of separation as agarose gel electrophoresis. For this case the samples are loaded into capillaries or microfluidic microchannels. Samples are detected by fluorescence and analyzed by commercial software developed to identify and quantify amount of each fragment in the sample.[36] This software evaluates the integrity of the sample and displays it as a standard value to facilitate comparison among samples. Depending of the vendor, commercially available equipment use different algorithms, such as artificial neural networks, to reach a standard value of integrity. This technique requires minimum amounts of sample and returns very accurate quantification values but suffers from high cost of equipment, making it not readily available for most small laboratories.

2.2 Hydrogel Microparticles

2.2.1 Properties

Hydrogels are networks of crosslinked hydrophilic polymer chains, which can be easily functionalized with different probes, i.e. nucleic acids.[27]

Hydrogels can be used in a wide range of biotechnology applications such as drug delivery, tissue engineering, and molecular diagnostic among others, due to their stable 3D porous network and hydrophilic environment that allows for improved interactions with target molecules.[37]

In this work, polyethylene glycol (PEG) (Fig. 4.A) hydrogels are used due to their biocompatibility, non-fouling character and their good solubility in aqueous buffers. Also, it is a relatively inexpensive material and allows for several chemical modifications. Specifically, poly(ethylene glycol)diacrylate (PEGDA) (Fig. 4.B), a common derivative of PEG that contain two acrylate groups, is used to prepare the PEG hydrogels structures via free-radical polymerization.

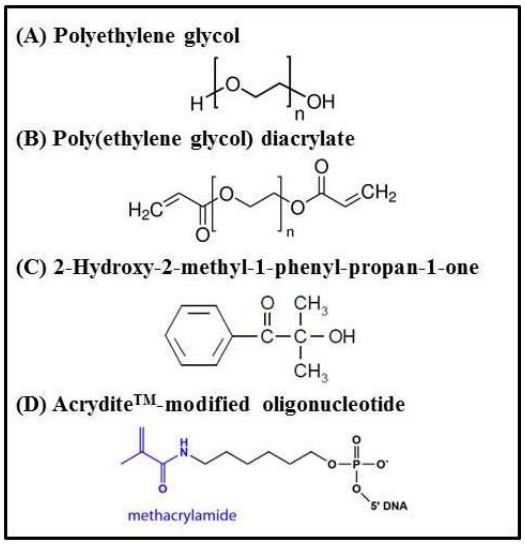

Fig.4. (A) Polyethylene glycol (B) Poly(ethylene glycol) diacrylate monomer (C) 2-Hydroxy-2-methyl-1-phenyl-propan-1-one (Darocur 1173 Photoinitiator) (D) Acrydite-modified oligonucleotide. This figure was adapted from Le Goff et al.[38]

2.2.2 Radical Chain Polymerization

Chain polymerization consists of three distinctive steps: initiation, propagation, and termination,[38] as seen in Fig. 5. In photoinitiated polymerizations the generation of reactive free radicals (R^*) is triggered by irradiating UV light to a photoinitiator (I), the free radical reacts with a monomer (M) to produce a new radical (M_1^*) that will lead the polymer growth by subsequently reacting with other monomers. The termination step occurs by two mechanisms. The first one is called bimolecular termination and involves the reaction of two propagating radical chains (coupling) and/or the addition of a hydrogen radical from one radical to another radical center to form two polymer chains (disproportionation). For the second mechanism, a free radical reacts with a reactive polymer chain to stop the growth of the chain. Inhibitors (Z) also react with growing polymer chains to stop the polymerization.[39]

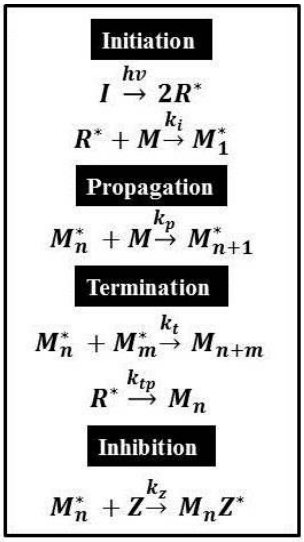

Fig. 5. General reaction mechanism for photoinitiated radical chain polymerizations. The reaction occurs through a sequence of four events: initiation, propagation, termination, and inhibition. This figure was reproduced from Lewis.[39]

2.2.3 Shape-Encoded Microparticles

One of the most important disadvantages of the traditional methods of fabrication of polymeric microparticles is the poor control over the shape and monodispersity, thus limiting their applicability. Photolithographic methods represent a good alternative for the fast and controllable production of shape-encoded polymeric microparticles. Fig. 6 shows some of the photolithography methods used to fabricate microparticles. While contact lithography and flow lithography (Fig. 6.A-B) offer direct and reliable production of microparticles, they suffer from certain limitations such as high cost of equipment and troublesome control of flow, respectively. Contrarily, replica molding technique (Fig. 6.C) presents several advantages including simple, robust, scalable and inexpensive procedures.[27] For this, a simple polymer preparticle solution is used to fill the wells of a PDMS elastomeric micromold, then the filled molds are exposed to UV light provided by a simple hand-held lamp. After polymerization hydrogel microparticles are easily recovered from the mold due to their swelling capacity.

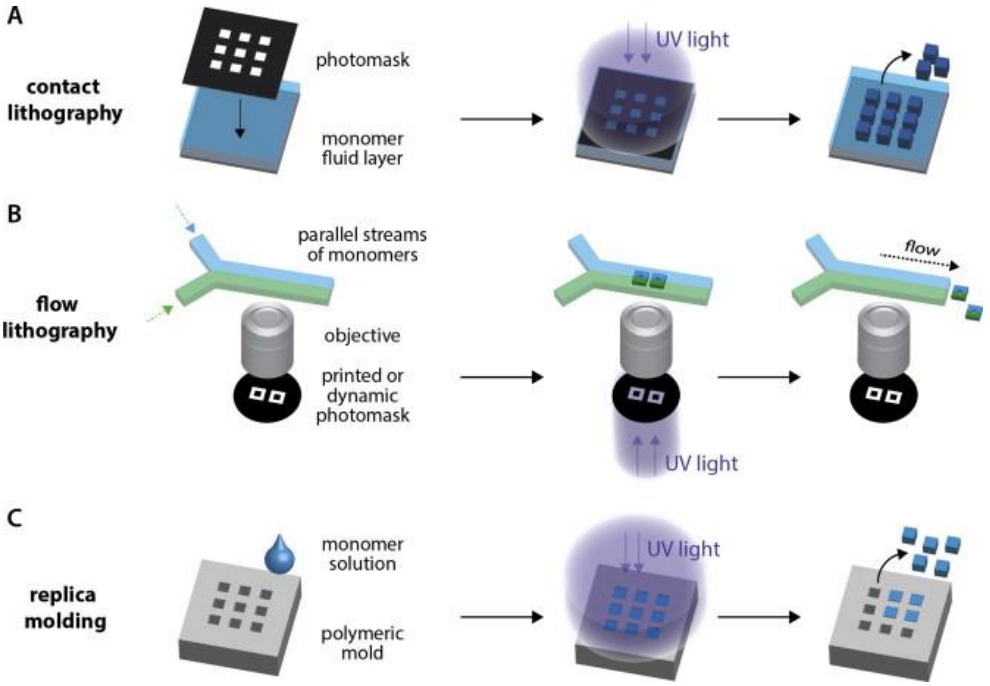

Fig. 6. Photolithography methods for microparticle production.(A) Contact lithography: uses a photomask in direct contact with the monomer solution. (B) Flow lithography: UV light is projected through photomasks to polymerize streams of monomers in microchannels. (C) Replica molding: monomer solutions are polymerized inside pre-designed molds. This figure was reproduced from Le Goff et al.[38]

Chapter 3: Materials and Methods

3.1 Reagents

Poly(ethylene glycol) PEG (M_w =600), poly(ethylene glycol) diacrylate (PEG-DA, M_n =700), 2-hydroxy-2-methylpropiophenone (Photoinitiator PI, Darocur 1173), Tris(hydroxymethyl) aminomethane (Trizma preset crystals, pH 7.5), saline sodium citrate (SSC) buffer (20x concentrate, molecular biology grade), 4-(2-Hydroxyethyl)piperazine-1-ethanesulfonic acid (HEPES, ≥99.5%), potassium chloride (99+%), aminoformamidinehydrochloride (Gu-HCl, molecular biology grade) and 2-Mercaptoethanol were purchased from Sigma-Aldrich (St. Louis, MO). Tween 20 (TW20), poly(dimethlsiloxane) (PDMS) elastomer kits (Sylgard 184), and gold-coated glass slides (BioGold, C09-5076-M20) were purchased from Thermo Fisher Scientific (Waltham, MA). YOYO-1 Iodide (Y3601) was purchased from Molecular Probes (Eugene, OR). Luria-Bertani (LB) Broth (tissue culture grade) was purchased from Amresco (Solon, OH). Lysozyme was purchased from MP Biomedicals (Solon, OH). All the purchased chemicals were used without further purification.

3.2 ssDNA oligonucleotides (probe and linker)

All the single stranded DNA oligonucleotides used in this study were purchased from Integrated DNA Technologies, Inc. (Coralville, IA) and used without further purification.

Probe ssDNA (5'-/acrydite/ATGATGATGATGATGATG-3'), mismatch probe (5'-/acrydite/CACTACCGATACGTACTCAG-3'), fluorescently labeled

(fluorescein isothiocyanate) target ssDNA (5'-/FITC/CATCATCATCATCATCAT-3'). Linker DNA's (16S: 5'-**GTCCCCCTCTTTGGTCTTGC***TTTTTT*CATCATCATCATCATCAT-3'; 23S: 5'-**AATCTCGGTTGATTTCTT***TTTTTT*CATCATCATCATCATCAT-3'), the linker DNA's were designed to contain **a region complementary to the target RNA molecules,**[28, 29] *a spacer* and a region complementary to the probe DNA incorporated in the microparticles.

3.3 *E. coli* Culture and Total RNA Preparation

Strain BL21 of *E. coli* cells housing the plasmid *pTrcHisB::gfpuv* were used to extract the RNA samples. Briefly, the cells were grown in 50 mL of Luria-Bertani (LB) media with ampicillin (50 µg/mL), and incubated at 37°C and 250 rpm. Samples were collected after 6 h (OD_{600}≈0.8). Total RNA samples were prepared using the Qiagen RNAprotect Bacteria Reagent and the Qiagen RNeasy Mini Kit according to manufacturer's manual. Briefly, cell samples were mixed with the RNAprotect reagent and centrifuged to cell pellet formation. Cells were then lysed with a lysozyme (1 mg/mL) solution in TE buffer for 5 min at room temperature. Cell lysate was then loaded to the RNeasy mini spin column. After RNA molecules bind to the column, multiple washing steps were performed and the total RNA sample was eluted with 50 µL of RNase-free water. The final concentration of the total RNA was measured using an Evolution 300 UV-vis spectrophotometer (Thermo Scientific, Waltham, MA) by measuring absorbance at 260 nm.

3.4 Microparticle Fabrication

PEG microparticles were fabricated via replica molding technique with minor modifications from previous report.[27] Briefly, the preparticle solutions consist of 15% (v/v) PEGDA, 35% (v/v) PEG 600, 2% (v/v) PI, probe DNA (50-200 μM final concentration), and TE buffer (10 mM Tris, pH 8.0, 1 mM EDTA) containing 0.02% (v/v) of 10% (w/w) sodium dodecyl sulfate (SDS). PDMS molds were fabricated by filling photolithographically patterned silicon master molds with Sylgard 184 and incubating them overnight at 65°C. The molds were filled with the prepolymer solution inside a humidity chamber (relative humidity higher than 90%) in order to minimize evaporation of water from the microwells (volume of each microparticle 400 pL). The filled mold was then sealed with a PDMS-coated glass slide (a square section of the coating was removed from the glass slide to provide a small gap). The sealed mold was then placed on an aluminum mirror (Thorlabs, Newton, NJ) and exposed to 365 nm UV light with an 8 W hand-held UV lamp (Spectronics Corp., Westbury, NY) for 30 min for photoinduced radical polymerization. After photopolymerization, the cross-linked microparticles were collected by placing water containing 0.5% (v/v) Tween 20 on the mold surface, physically bending the mold and by pipetting the content into a microcentrifuge tube.

In order to confirm the incorporation of the probe DNA, microparticles were first examined for DNA-DNA hybridization with fluorescein-labeled ssDNA targets. Briefly, the microparticles were mixed with 200 nM target DNA and

incubated at room temperature for 30 min on a rotator. After hybridization, microparticles were analyzed by fluorescence microscopy.

3.5 RNA Capture Assay

For the results shown in Fig. 7 and Fig. 8, total RNA samples were pre-incubated in a water bath with 2 μM 16S linker DNA at 30°C for one hour. These samples were then incubated with YOYO-1 dye at room temperature for 10 min, with 0.01 ratio of dye to base (d/b).[40] These pre-incubated samples were purified to remove all unreacted linker DNA and YOYO-1 dye using an RNA binding solution (5M Gu-HCl, 30% Isopropanol) and the Qiagen RNeasy mini column. 15% PEGDA microparticles are washed twice with 20 mM HEPES buffer (pH 7.4, 100 mM KCl), and then mixed with the total RNA samples in a final assay volume of 100 μL. These assay mixtures were incubated for 2 hours at 30°C in a water bath with occasional mixing every 20 min. After incubation, the microparticles were analyzed by fluorescence microscopy. Agarose gel electrophoresis images of the samples throughout the assay are shown in Fig. S1.

3.6 Multiplex Assay

Microparticles with three different shapes were fabricated based on the same preparticle solution, and were designated for negative control, 16S rRNA and 23S rRNA capture These microparticles were incubated for 30 min at 30°C with no linker DNA, 2 μM 16S linker DNA and 2 μM 23S linker DNA, respectively. Total RNA samples were incubated with YOYO-1 dye at room temperature for 10 min and then purified using the Qiagen RNeasy Mini Kit.

Finally, mixtures of each three of microparticles were incubated with the total RNA sample complexed with YOYO-1 in a final volume of 100 µL for 2 hours at 30°C. To analyze RNA stability, the assay is repeated with total RNA complexed with YOYO-1 that were stored for 2, 4 and 5 days. The microparticles were then analyzed by fluorescence microscopy.

3.7 Image Analysis

Microparticles were imaged using an Olympus BX51 microscope equipped with a standard green filter set U-N31001 (Chroma Technology Corp., Rockingham, VT) and a DP70 microscope digital camera to capture the fluorescence micrographs. All the measurements of fluorescence intensities were examined for at least 5 particles per condition and evaluated using ImageJ software.[41]

3.8 Equilibrium Binding Model

The equilibrium binding model utilized to describe the relationship between the ssDNA probes (P) available for binding in the microparticles and the target RNA molecules (T) pre-conjugated with linker DNA and YOYO-1 dye as previously described:[24]

$$T + P \leftrightarrow TP$$

Briefly, TP represents the complex formed by the capture probe and the complex YOYO-RNA-linker DNA. The equilibrium is characterized by the dissociation constant K_{d}:

$$K_{\mathrm{d}} = \frac{[T][P]}{[TP]}$$

Starting with the assumption that the concentration of TP complex is directly proportional to the fluorescence intensity ($[TP] = k[F.I.]$) and replacing this into the equilibrium binding relationship, I obtained the following equation:

$$[F.I.] = \left(\frac{1}{k}\right)\frac{[P]_0[T]}{K_{\mathrm{d}} + [T]} = \frac{k'[T]}{K_{\mathrm{d}} + [T]}$$

Where $[P]_0$ represents the maximum concentration of probe DNA available for binding, consequently *k'* represents the maximum fluorescence intensity of particles after rRNA capture. In order to evaluate the constants K_{d} and k', a double reciprocal plot was utilized:

$$\frac{1}{[F.I.]} = \frac{K_d}{k'[T]} + \frac{1}{k'}$$

Values for k' and K_{d} obtained in my study were 9.8 AU and 5.9 µg/mL respectively.

Chapter 4: Results and Discussion

4.1 Sequence Specificity and Reliability

As shown in Fig. 7, I first demonstrate sequence-specific, simple amplification-free assay of bacterial rRNA molecules with capture DNA-conjugated microparticles. For this, I used a replica molding technique to fabricate shape-encoded microparticles containing 15% (v/v) poly(ethylene glycol) diacrylate (PEGDA) and probe single stranded (ss) DNA (50, 100 and 200 μM). These particles were incubated with total RNA samples from an *E. coli* culture and pre-conjugated with 16S linker DNA and YOYO-1 dye. The particles were imaged with a fluorescence microscope, and the average fluorescence intensity was measured at the center region of at least 5 particles per condition.

First, the fluorescence micrographs and their corresponding bright-field micrographs (insets) in Fig. 7.A-C (top row) show that the particles are highly uniform with well-defined shapes, indicating the robustness of the simple replica molding-based fabrication. Next, the fluorescence intensity increases with increasing probe DNA concentration, while the fluorescence among particles with the same probe DNA concentration is consistent, indicating reliable assay.

Next, the background-subtracted fluorescence plot of Fig. 7.D from image analysis of the results in Fig. 7.A-C confirms that higher probe DNA content in the prepolymer mixture leads to higher fluorescence upon rRNA binding. Specifically, there is a 40% increase in the fluorescence for particles with 200 μM

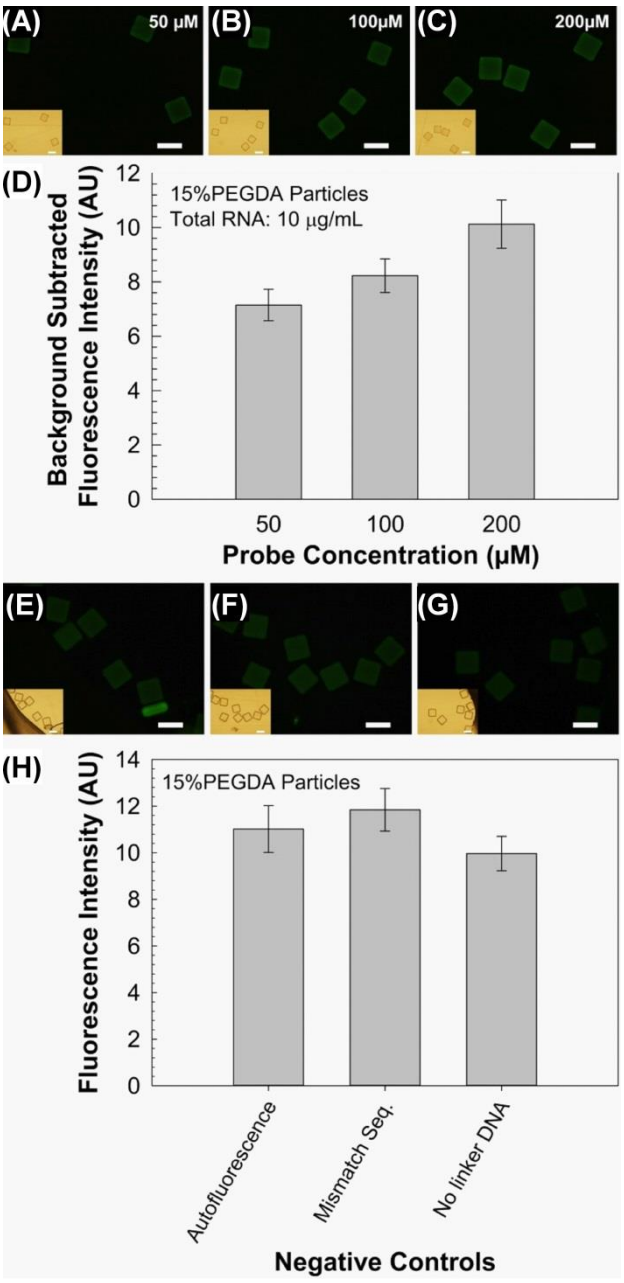

Fig. 7. Analysis of Sequence Specificity and Reliability. (A-C) Fluorescence micrographs of microparticles, with 50, 100 and 200 µM probe DNA concentration respectively, upon total RNA assay. (D) Plot of background-subtracted fluorescence intensity for each set of particles in A-C. (E-G) Negative Controls: Fluorescence micrographs for microparticles' autofluorescence, microparticles with mismatch sequence, and microparticles incubated with RNA without linker DNA respectively. (H) Plot of average fluorescence intensity for each set of particles in E-G. Scale bars represent 100 µm.

probe DNA compared to particles with only 50 μM probe DNA. The consistently small error bars for all conditions indicates the consistency of the rRNA assay.

Note, four-fold increase in the probe DNA did not lead to four-fold increase in the fluorescence. I attribute this non-stoichiometric behavior to two possible sources. First, the probe DNA incorporation efficiency for each case may be different due to the effect of the low percentage of PEGDA during polymerization, leading to inefficient polymerization and conjugation yield.[42] Second, the large size of rRNA molecules may prevent their diffusion and binding with the available probe DNA across the microparticles. Specifically, the 16S RNA has 1542 nucleotides, thus has the molecular weight of 520kDa, hydrodynamic radius R_h of approximately 12.5 nm[43] and radius of gyration R_g of 8.5 nm.[44] Compared to this large rRNA size, the mesh size of the microparticles fabricated with 15% PEGDA is expected to be smaller (average pore size ~1 nm),[45] limiting the access and mass transfer of the rRNA targets through the microparticles.

Next, I examined three negative control conditions to confirm the sequence-specific nature of the assay as shown in Fig. 7.E-H. The first set (Fig. 7.E) corresponds to the autofluorescence of the microparticles[46] without incubation with RNA samples. The second set (Fig. 7.F) represents a mismatching sequence, where the microparticles are fabricated using a non-complementary sequence of probe DNA (mismatch probe, Materials and Methods) from the linker DNA sequence. The third set (Fig. 7.G) corresponds to microparticles incubated with a complex of RNA and YOYO-1 dye only, without the linker DNA. Average

fluorescence intensities for all the three negative control conditions are consistently low compared to the matching conditions shown in Fig. 7.A-C, indicating the sequence specific nature of the assay with minimal nonspecific binding between the microparticles and the RNA complexes, in addition the short duration of the assay confirms the rapid and selective binding nature of the hybridization reaction. Moreover, these results confirm the accessibility of the rRNA sequences for hybridization with the linker DNA sequences under the non-denaturing conditions of the assay, further confirming results by Fuchs *et al*.[30] In summary, the results in Fig. 6 indicate that this simple microparticle suspension array-based rRNA assay is reliable and sequence-specific.

4.2 Microparticle Responsiveness to Target Total RNA Concentration

Next, I examined the responsiveness and sensitivity of the DNA-conjugated microparticles and the assay method to the target RNA concentration, as shown in Fig. 8. For this, I utilized the microparticles fabricated with 15% PEGDA-200uM probe DNA as shown in Fig. 7, and exposed them to various concentrations of total RNA samples that are pre-incubated with linker DNA and YOYO-1 dye.

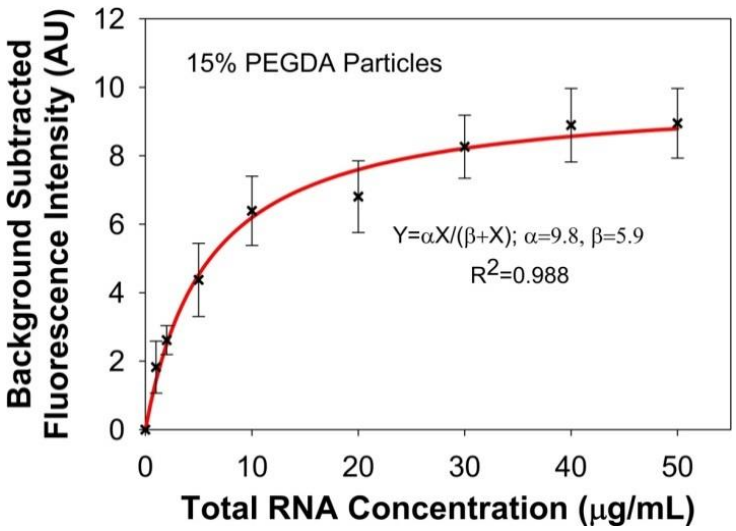

Fig. 8. Plot of average background-subtracted fluorescence intensity vs. total RNA concentration. The solid curve represents the equilibrium binding model, quantified by the equilibrium binding model equation.

First, the background-subtracted fluorescence of the microparticles show a typical saturation (or Langmuir isotherm) type behavior, as shown in Fig. 8. This result indicates that the microparticle-based assay is responsive to the target RNA concentration. Next, the fluorescence micrographs show uniformity among all the center regions of microparticles as represented by the error bars, which are consistently small in all the conditions examined, indicating reliability of my method. Third, 1 μg/mL total RNA concentration is readily detectable.

I then utilized a Langmuir isotherm-type data fitting to examine the binding behavior, and shown in the curve of Fig. 8 (Materials and Methods). The binding behavior appears to follow the typical saturation behavior with high R^2 value of 0.988, suggesting reliability and equivalent access of the rRNA targets to the binding sites. In short summary, results shown in Fig. 8 indicate that this

simple microparticle suspension array method provides responsive binding behavior to the target concentrations in complex total RNA samples.

4.3 Multiplexed rRNA Stability Assay

Finally, I examined the relative stability of 16S and 23S rRNAs from total RNA samples using simple shape-encoded multiplexing scheme, as shown in Fig. 9. Specifically, the simple replica molding allows fabrication of microparticles with various 2D geometries in a reliable and high-fidelity manner to 20μm size ranges without the need for complex fluidic control, equipment or multistep procedures.[47, 48] In this work, I fabricated microparticles with three different shapes as shown in the schematic diagram of Figure 9.A; particles with the square shape in the leftmost diagram in Fig. 9.A are used as negative control, the middle diagram for 16S rRNA capture, and the rightmost diagram for 23S rRNA capture. Each set of particles is then incubated with no linker DNA, 16S linker DNA and 23S linker DNA respectively. Mixtures of these three types of microparticles were then exposed to the total RNA samples complexed with YOYO-1 upon storage at room temperature at various times; immediately after or two, four and five days after the RNA extraction.

First, the brightfield micrograph of Fig. 9.B shows the three types of the microparticles with well-defined shapes, indicating the consistency of the simple shape-controlled fabrication technique. Next, the fluorescence micrograph of Fig. 9.C clearly shows lower fluorescence intensity for the negative control particles, while the other two types specific for 16S and 23S RNAs respectively show

equivalent fluorescence. The 23S rRNA has about twice the size than 16S rRNA (23S: 2904 nt, ~ 990 kDa). Yet, due to the larger size, less 23S rRNA is expected to be captured on the surface of the microparticles. In short summary, this fluorescence result confirms this simple multiplexed assay scheme.

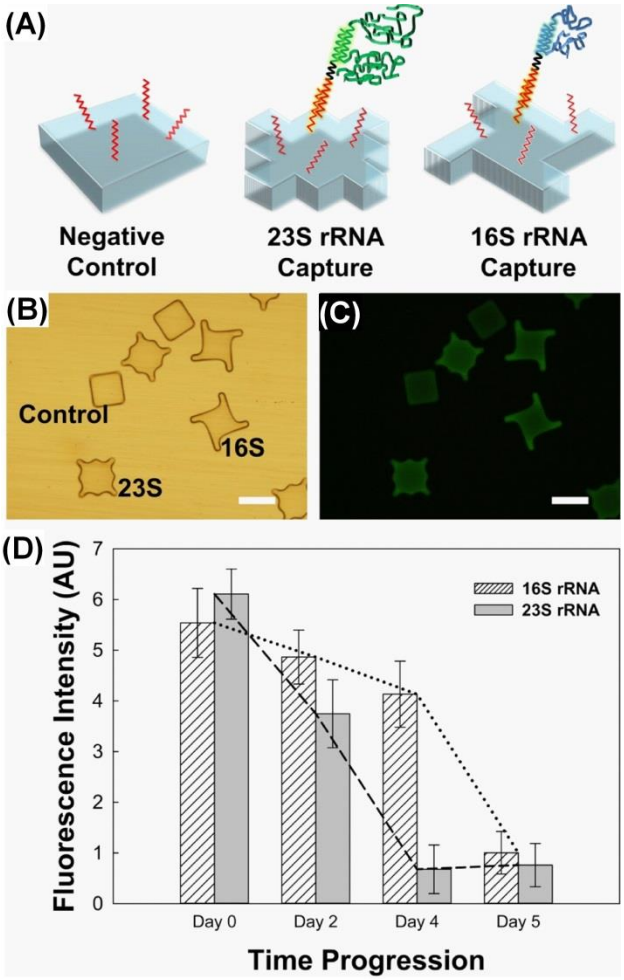

Fig. 9. Multiplexed Assay. (A) From left to right: design of shape-encoded microparticles used for negative control, 16S rRNA capture, and 23S rRNA capture respectively. (B-C) Brightfield and fluorescence micrograph respectively, showing the microparticles described in A upon a multiplexed assay. (D) Plot of the average background-subtracted fluorescence intensity vs. time progression for 16S rRNA (dashed columns) and 23S rRNA (gray columns) samples. Degradation progress is shown for 16S rRNA (dotted line) and 23S rRNA (dashed line). Scale bars represent 100 µm.

Finally, I examined the stability of the two rRNAs over five days' period of storage as shown in Fig. 9.D. First, 16S rRNA (dashed columns) remained relatively stable for four days, with about 75% fluorescence remaining after four days at room temperature (dotted line). In contrast, 23S rRNA (gray columns) started degrading rapidly, with less than 11% florescence remaining after four days (dashed line). After five days, 16S rRNA degraded to the level of 23S rRNA based on the fluorescence. These results are consistent with the expected relative stability of the two rRNAs. Specifically, 16S rRNA is known to be more stable than 23S rRNA, while the degradation is expected to occur rapidly once the process initiates.[33, 49] All the microparticle assay results were also confirmed with agarose gel electrophoresis of the degraded RNA samples (Fig. S2). In short summary, the results in Fig. 9.D confirms the utility of this simple multiplexed microparticle suspension arrays in rRNA stability assay from complex total RNA samples. Meanwhile, the error bars for all the conditions examined were relatively small, further confirming the reliability of the simple shape-encoded multiplexed assay scheme.

In summary, the results in Fig. 9 demonstrates reliable rRNA stability assay from complex total RNA samples using simple shape-encoded microparticle arrays.

Chapter 5: Conclusion and Future Directions

In this work, I enlisted a simple sandwich assay-type method to examine bacterial rRNA titer and RNA sample integrity using a 16S/23S rRNA pair. Robust replica molding was utilized to fabricate capture DNA-containing microparticles with simple shape encoding for multiplexed assays. The results showed sequence-specific and responsive binding behavior to complex total RNA samples, as well as reliable evaluation of the RNA decay profile under standard fluorescence imaging conditions without sample amplification or complex equipment. Further enhancements in the fluorescence intensity, sensitivity and signal-to-noise ratio could be readily achieved with improved particle fabrication and compositions as well as signal amplification methods.[25, 47] More efficient capture DNA incorporation and accessibility through inert porogens and other polymerizable monomers are currently being pursued.

Supplementary Materials

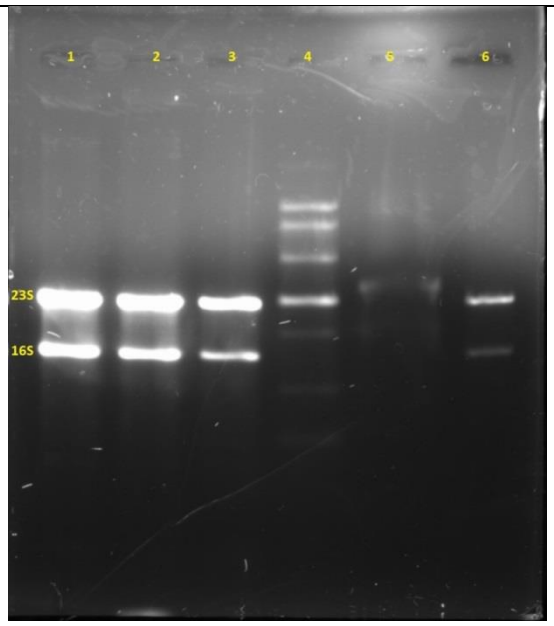

Fig. S1. Agarose gel for confirmation of total RNA extraction and presence throughout the assay. Lane1: Extracted total RNA, Lane 2:RNA incubated with linker DNA, Lane 3: RNA + linker DNA+ YOYO-1 (before purification), Lane 4:RNA ladder, Lane 5: Eluent from purification, Lane 6: RNA + linker DNA + YOYO-1 (after purification)

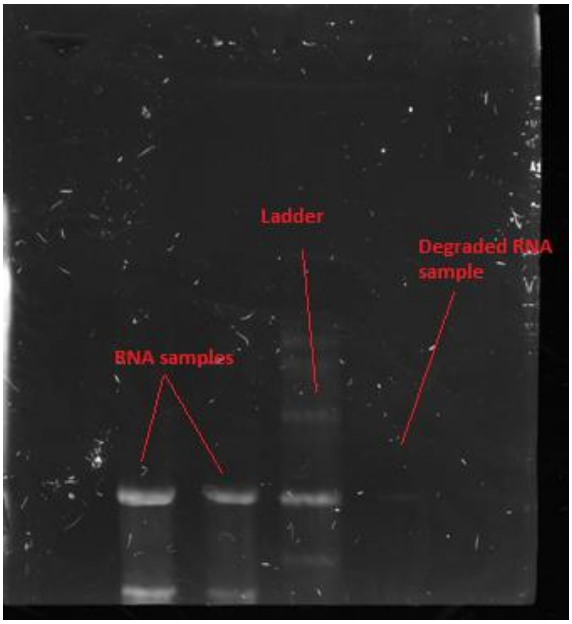

Fig. S2. Agarose gel showing degradation rRNA through time. Total degradation occurs after 5 days of incubation at room temperature.

References

1. Fleige, S. and M.W. Pfaffl, *RNA integrity and the effect on the real-time qRT-PCR performance.* Molecular Aspects of Medicine, 2006. **27**(2–3): p. 126-139.
2. Ramaswamy, S. and T.R. Golub, *DNA Microarrays in Clinical Oncology.* Journal of Clinical Oncology, 2002. **20**(7): p. 1932-1941.
3. Copois, V., et al., *Impact of RNA degradation on gene expression profiles: Assessment of different methods to reliably determine RNA quality.* Journal of Biotechnology, 2007. **127**(4): p. 549-559.
4. Vermeulen, J., et al., *Measurable impact of RNA quality on gene expression results from quantitative PCR.* Nucleic Acids Research, 2011. **39 (9)**.
5. Gopinath, S.C.B., et al., *Bacterial detection: From microscope to smartphone.* Biosensors and Bioelectronics, 2014. **60**(0): p. 332-342.
6. Ares, M., *Bacterial RNA Isolation.* Cold Spring Harb Protoc, 2012(9).
7. Thatcher, S.A., *DNA/RNA Preparation for Molecular Detection.* Clinical Chemistry, 2015. **61**(1): p. 89-99.
8. Becker, C., et al., *mRNA and microRNA quality control for RT-qPCR analysis.* Methods, 2010. **50**(4): p. 237-243.
9. Die, J.V. and B. Román, *RNA quality assessment: a view from plant qPCR studies.* Journal of Experimental Botany, 2012. **63**(17): p. 6069-6077.
10. Manchester, K.L., *Use of UV methods for measurement of protein and nucleic acid concentrations.* Biotechniques, 1996. **20**(6): p. 968-70.
11. Sambrook, J. and D. Russell, *Molecular Cloning: A Laboratory Manual*. 3rd ed, ed. C.S. Harbor. 2001, NY, USA.: Cold Spring Harbor Laboratory Press.
12. Imbeaud, S., et al., *Towards standardization of RNA quality assessment using user-independent classifiers of microcapillary electrophoresis traces.* Nucleic Acids Research, 2005. **33**(6): p. e56.
13. Schroeder, A., et al., *The RIN: an RNA integrity number for assigning integrity values to RNA measurements.* BMC Molecular Biology, 2006. **7**: p. 3-3.
14. Denisov, V., et al., *Development and validation of RQI: an RNA quality indicator for the Experion™ automated electrophoresis system* in *Tech Note*. 2008, Bio-Rad.
15. Breadmore, M.C., *Capillary and microchip electrophoresis: Challenging the common conceptions.* Journal of Chromatography A, 2012. **1221**(0): p. 42-55.
16. Duy, J., et al., *A field-deployable colorimetric bioassay for the rapid and specific detection of ribosomal RNA.* Biosensors and Bioelectronics, 2014. **52**(0): p. 433-437.
17. Aslan, K., et al., *Metal-Enhanced Fluorescence-Based RNA Sensing.* Journal of the American Chemical Society, 2006. **128**(13): p. 4206-4207.

18. Foudeh, A.M., et al., *Sub-femtomole detection of 16s rRNA from Legionella pneumophila using surface plasmon resonance imaging.* Biosensors and Bioelectronics, 2014. **52**(0): p. 129-135.
19. Auer, H., et al., *Chipping away at the chip bias: RNA degradation in microarray analysis.* Nat Genet, 2003. **35**(4): p. 292-293.
20. Wilkes, T., et al., *Evaluation of a novel approach for the measurement of RNA quality.* BMC Research Notes, 2010. **3**(1): p. 89.
21. Tjong, V., et al., *Direct Fluorescence Detection of RNA on Microarrays by Surface-Initiated Enzymatic Polymerization.* Analytical Chemistry, 2013. **85**(1): p. 426-433.
22. Squires, T.M., R.J. Messinger, and S.R. Manalis, *Making it stick: convection, reaction and diffusion in surface-based biosensors.* Nature Biotechnology, 2008. **26**(4): p. 417-426.
23. Feldman, A.L., et al., *Advantages of mRNA amplification for microarray analysis.* Biotechniques, 2002. **33**(4): p. 906-12, 914.
24. Pregibon, D.C., M. Toner, and P.S. Doyle, *Multifunctional Encoded Particles for High-Throughput Biomolecule Analysis.* Science, 2007. **315**(5817): p. 1393-1396.
25. Choi, N.W., et al., *Multiplexed Detection of mRNA Using Porosity-Tuned Hydrogel Microparticles.* Analytical Chemistry, 2012. **84**(21): p. 9370-9378.
26. Rehman, F.N., et al., *Immobilization of acrylamide-modified oligonucleotides by co-polymerization.* Nucleic Acids Research, 1999. **27**(2): p. 649-655.
27. Lewis, C.L., et al., *Fabrication of Uniform DNA-Conjugated Hydrogel Microparticles via Replica Molding for Facile Nucleic Acid Hybridization Assays.* Analytical Chemistry, 2010. **82**(13): p. 5851-5858.
28. Fuchs, B.M., et al., *In Situ Accessibility of Escherichia coli 23S rRNA to Fluorescently Labeled Oligonucleotide Probes.* Applied and Environmental Microbiology, 2001. **67**(2): p. 961-968.
29. Nelson, B.P., et al., *Label-free detection of 16S ribosomal RNA hybridization on reusable DNA arrays using surface plasmon resonance imaging.* Environmental Microbiology, 2002. **4**(11): p. 735-743.
30. Fuchs, B.M., et al., *Flow Cytometric Analysis of the In Situ Accessibility of Escherichia coli 16S rRNA for Fluorescently Labeled Oligonucleotide Probes.* Applied and Environmental Microbiology, 1998. **64**(12): p. 4973-4982.
31. Nielsen, H., *Working with RNA*, in *RNA*, H. Nielsen, Editor. 2011, Humana Press. p. 15-28.
32. Moore, P.B. and T.A. Steitz, *The Roles of RNA in the Synthesis of Protein.* Cold Spring Harbor Perspectives in Biology, 2011. **3**(11).
33. Li, Z. and M.P. Deutscher, *Analyzing the Decay of Stable RNAs in E. coli.* Methods in Enzymology, 2008. **Volume 447**: p. 31-45.
34. UCSC. Available from: http://rna.ucsc.edu/.

35. Schneider, D.A., W. Ross, and R.L. Gourse, *Control of rRNA expression in Escherichia coli.* Current Opinion in Microbiology, 2003. **6**(2): p. 151-156.
36. Zhong, W. and E.S. Yeung, *High-Throughput Analysis of Total RNA Expression Profiles by Capillary Gel Electrophoresis.* Analytical Chemistry, 2003. **75**(17): p. 4415-4422.
37. Peppas, N.A., et al., *Hydrogels in Biology and Medicine: From Molecular Principles to Bionanotechnology.* Advanced Materials, 2006. **18**(11): p. 1345-1360.
38. Le Goff, G.C., et al., *Hydrogel microparticles for biosensing.* European Polymer Journal, (0).
39. Lewis, C.L., *Novel Fabrication Strategies for Multifunctional Hydrogel Particles*. 2011, Tufts University: Ann Arbor. p. 143.
40. Carlsson, C., M. Jonsson, and B. Akerman, *Double bands in DNA gel electrophoresis caused by bis-intercalating dyes.* Nucleic Acids Research, 1995. **23**(13): p. 2413-2420.
41. Rasband, W.S. *ImageJ*. 1997-2014 [cited 2015; 1997-2014]. Available from: http://imagej.nih.gov/ij/.
42. Pregibon, D.C. and P.S. Doyle, *Optimization of Encoded Hydrogel Particles for Nucleic Acid Quantification.* Analytical chemistry, 2009. **81**(12): p. 4873-4881.
43. Tam, M.F., J.A. Dodd, and W.E. Hill, *Physical characteristics of 16 S rRNA under reconstitution conditions.* J Biol Chem, 1981. **256**(12): p. 6430-4.
44. Yoffe, A.M., et al., *Predicting the sizes of large RNA molecules.* Proceedings of the National Academy of Sciences of the United States of America, 2008. **105**(42): p. 16153-16158.
45. Mellott, M.B., K. Searcy, and M.V. Pishko, *Release of protein from highly cross-linked hydrogels of poly(ethylene glycol) diacrylate fabricated by UV polymerization.* Biomaterials, 2001. **22**(9): p. 929-941.
46. Chiu, Y.C., E. Brey, and V. Pérez-Luna, *A Study of the Intrinsic Autofluorescence of Poly (ethylene glycol)-co-(L -Lactic acid) Diacrylate.* Journal of Fluorescence, 2012. **22**(3): p. 907-913.
47. Lee, A.G., et al., *Development of Macroporous Poly(ethylene glycol) Hydrogel Arrays within Microfluidic Channels.* Biomacromolecules, 2010. **11**(12): p. 3316-3324.
48. Dendukuri, D., et al., *Stop-flow lithography in a microfluidic device.* Lab on a Chip, 2007. **7**(7): p. 818-828.
49. Deutscher, M.P., *Degradation of Stable RNA in Bacteria.* Journal of Biological Chemistry, 2003. **278**(46): p. 45041-45044.